

# Analysis of Heart Rate Variation Filtering Using LMS Based Adaptive Systems

S. SEYEDTABAII

Electrical Engineering Department

Shahed University

Tehran

IRAN

[stabaii@shahed.ac.ir](mailto:stabaii@shahed.ac.ir)

*Abstract:* - Heart Rate Variability (HRV) is widely used as an index of human autonomic nervous activity. HRV is composed of two major components: high frequency respiratory sinus arrhythmia (RSA) and low frequency sympathetic components. The ratio of LF/HF is viewed as an index of human autonomic balance, so the low frequency sympathetic and the high frequency parasympathetic components of an ECG R-R interval must be adequately separated. Adaptive filters can isolate the low frequency, enabling the attainment of more accurate heart rate variability measures. For the raised case, this paper suggests an efficient (short size) case based model and illustrates its performance in adaptive filtering of heart rate signal. This method renders analogous results to what a higher order conventional FIR model adaptive filter may yield. The strength of the proposed model comes out of its ability in tracking the phase difference variation between the reference and the main signal of an adaptive filtering system. This capability, then is shown, that leads to the increase in the convergence rate of the LMS algorithm in HRV adaptive filtering. Simulation results supporting the proposed concept are presented.

*Key-Words:* - Adaptive filter, All pass filter, FIR model, First order equalizer, HRV filtering, Rate of convergence, Least Mean Squares.

## 1 Introduction

Heart rate variability (HRV) is a measure of alterations in heart rate derived by measuring the variation of RR intervals. HRV parameters have been shown to aid assessment of cardiovascular disease [1]. Heart rate is influenced by both sympathetic and parasympathetic (vagal) activity. The influence and balance of both branches of the autonomic nervous system (ANS) have been termed sympathovagal balance and is reflected in the RR interval changes. A low frequency (LF) component of HRV has been proposed as reflecting both sympathetic and parasympathetic effects on the heart and generally occurs in a band between 0.04 Hz and 0.15 Hz. The influence of vagal efferent modulation of the sinoatrial node can be seen in the high frequency band (HF), loosely defined between 0.15 and 0.4 Hz and known as respiratory sinus arrhythmia (RSA) because it occurs at the respiratory frequency. The magnitude of this high frequency band has been demonstrated to be associated with the extent of cardiac parasympathetic activity in pharmacological autonomic blockade studies [3], respiratory sinus arrhythmia, cardiac vagal tone, and respiration: within and between-individual relations.

The ratio of power in the LF and HF components (LF/HF) has been used to provide an estimate of cardiac sympathovagal balance, although this measure remains indispute [2]. Nevertheless, several studies have indicated that when considered jointly, HF and LF HRV may provide useful information about both sympathetic and parasympathetic influences upon the cardiac cycle [4].

Spectral HRV is a measure of power in various frequency bands. To determine the RSA amplitude over a period of time, frequency domain, time domain and phase domain approaches have been analyzed [6]. Presented in [5] is an adaptive filter that separates the LF and HF components and therefore yields distinct spectral analysis measures for each band. The suggested order for the used FIR filter is 20. In this paper an adaptive filter with a new model structure, with just a few parameters, is introduced which behaves similar to the higher order FIR model adaptive filter in facing RSA filtering. The reason behind the power of this model is its capability in offering a higher rate of convergence to the adaptive algorithm. When the unwanted and the main signal have close frequency bands, the

algorithm with higher rate of convergence perform superior to the other contestant's algorithms.

In section 2 the high frequency component of HRV signal is briefly analyzed. Section 3 embodies a short description of adaptive filter and the basis of the proposed model. Section 4 contains simulation results and finally, conclusion comes in section 5.

## 2 HF HRV signal analysis

In this section, the process of respiratory pattern effect on HRV is investigated. Understanding the relationship between the breathing signal and the high frequency parasympathetic components of HRV surely directs us to finding a better and computationally efficient method for the decomposition of HRV into its low and high frequency components.

In the recent years, there has been a lot of research efforts regarding heart rate variability (HRV) mechanisms. A search, made in PubMed, reported more than 4,000 citations that both linear and nonlinear HRV measures had been used [11]. Mostly, linear estimates, which include various time and frequency domain indices, was used for the HRV measurement. However, a few non-linear indices of HRV had also been proposed [11].

HRV signal contains 3 frequency bands [11]:

- A very low frequency (VLF) band located in the less than 0.04 Hz (with dubious physiologic significance).
- A low frequency (LF) band located in the 0.04-0.15 Hz range (which derives from short term regulation of blood pressure).
- A high frequency (HF) band with a very large range from 0.15-0.40 Hz (reflecting momentary respiratory influences on the heart rate or respiratory sinus arrhythmia)

The respiratory parameters that can affect HRV estimates, include respiratory frequency, tidal volume, end tidal partial pressure of carbon di-oxide (PETco<sub>2</sub>), the time ratio of expiration/inspiration and respiratory dead space [11]. Since breathing through an oro-nasal mask or mouthpiece can also affect breathing pattern, it can be extrapolated that it will also influence HRV estimates [11].

### 2.1 HF HRV Frequency

Simultaneous oscillation of heart rate (HR) and blood pressure (BP) at the breathing frequency was first observed by Hales in 1733. The respiration related fluctuation of HR has been named "respiratory sinus arrhythmia" (RSA), and it manifests as

increasing HR upon inspiration and decreasing HR upon expiration [7]. On the other hand, parallel oscillation of RR intervals with nerve activity in the absence of lung movements have also been reported [8] that indicates the association between the central respiratory drive and respiratory-related cardiovascular oscillation, thus, it would be wise to regard HRV oscillation even in the absence of lung movement.

Related to the importance of respiration, the logical conclusion is that once the actual breathing rate is known, detection of the HF power should be centered around the fundamental respiration frequency and not a default fixed frequency which is the case with traditional HRV analysis. This also implies that breathing pattern ( $V_t$ ) is a good signature for removal of HF component from HRV.

Noting that, since the measured breathing pattern signal is not a pure sinusoid and contains harmonics of its fundamental frequency, for having an appropriate reference signal, the  $V_t$  fundamental frequency has to be extracted. This is also true for the measured RR interval signal containing RSA and its fundamental frequency harmonics.

- **Cardiac aliasing**

There is yet another mechanism reported to be involved in mediating respiratory fluctuations of heartbeat. [12] observed that if a special relationship exists between mean heart rate (fHR) and mean frequency of breathing (fB) such that fB is greater than 1/2 fHR, RSA can be observed in a frequency range which is lower than the frequency of breathing. The mathematical fundamentals of this physiological phenomenon are the same as those for the 'aliasing' effect in signal sampling [11]. However, the rate of breathing showing this phenomenon, is actually higher than the normal one and this can only happen in special test procedures.

- **Low frequency component**

Recently, independence of low-frequency rhythms from respiratory activity has also been reported [11].

- **Respiratory frequency change**

Frequency modulation breathing yields a large LF/HF index as predicted from the theoretical analysis and from simulated data [13]. Free breathing yields even larger values for the LF/HF index than FM breathing, which is consistent with the large variability in breathing patterns when subjects are allowed to breathe at will [13]. This result means that HF power spectrum is widened by variation in breathing frequency.

## 2.2 RSA Amplitude

- **Respiratory frequency**

Despite many past studies, the precise mechanisms of respiration-induced SA are still debated [11]. However, the RSA amplitude is markedly affected by respiratory frequency [15]. As the respiratory frequency decreases, the RSA amplitude increases to attain a maximum amplitude at  $6\text{min}^{-1}$ , and as the frequency goes below  $6\text{min}^{-1}$ , the amplitude decreases [15, 10].

In an experiment reported in [14], HF power at a respiration rate of  $15\text{min}^{-1}$  was increased compared with the other rates. LF power, in turn, was relatively small at that physiologic rate, so that the measurement of sympathetic/parasympathetic balance, was close to unity. Reductions of respiration rate shifted the RSA into LF range or even below LF range. In accordance with this shift, LF power was increased whereas HF power was reduced, resulting in an increased ratio of HF to LF power. The respiration rate of  $30\text{min}^{-1}$  was also associated with reduced HF power, because, at this rate, the RSA falls beyond the HF range. This led, together with the almost unchanged LF power, to a non-significant increase in LF/Hf, erroneously suggesting a changed sympatho-vagal balance. LF power tended to decrease from below a rate of  $6\text{min}^{-1}$ . Once the RSA is equal to power in a frequency band around respiratory rate, it can shift throughout the spectrum depending on the respiration and thus, obscure the effects under investigation. This results are in good accordance with results from other studies that showed that the amount of the RSA-related power in the frequency domain varies with the respiration rate: it is high at low rates and starts to decrease at a rate of about  $7\text{min}^{-1}$ .

Multiple regression analyses of RSA as criterion variable and respiratory measures (frequency and tidal volume) as predictors confirmed that RSA magnitude was significantly associated with respiratory parameters during daily life [17].

- **Tidal volume**

In a synchronized breathing-heart beat test, [9] reports that there are no statistically significant heart rate changes with the doubling of the tidal volumes, thus, implies that variations occurring with normal breathing should not seriously change HRV, whereas, [16] shows a change of about 20% in HRV with similar tidal volume changes. In another respiratory frequency controlled experiment reported in [15], it is shown that there is an approximately linear relationship between RSA and tidal volume

both in 0.1 Hz and 0.25 HZ which linearity is more consistent in 0.25 Hz than in 0.1 Hz. The conclusion is that there is a sort of relationship between tidal volume amplitude and RSA amplitude.

- **HRV amplitude versus  $\text{CO}_2$**

It has been shown in conscious humans [7] that increase in RSA magnitude due to the direct effects of  $\text{CO}_2$  are independent of changes in tidal volume and breathing frequency [11].

- **Relative timing of inspiration and expiration**

[18] showed that RSA could also be modulated by a third respiratory variable. In their experiment, examining the effect of a variation in inspiration and expiration times on heart rate variability, the subjects were given controlled breathing with either short inspiration followed by long expiration or long inspiration followed by short expiration. In trials with short inspiration followed by long expiration, RSA was significantly larger than in trials with long inspiration followed by short expiration [11].

- **Respiratory dead space**

Result of an experiment suggests that the power spectrum of heart rate variability is strongly influenced by the dead space induced by a face mask used in expiratory gas exchange analysis [11].

- **Age**

The results of study in [9] showed a significant decrease in HRC with increasing age.

## 2.3 RSA Phase shift

The results of a synchronized respiration-heart beat experiment shows that there is a variable phase shift between the HF HRV signal and the respiratory signal ( $V_t$ ) that changes when subject shifts from sitting position to supine position [9]. [10] also measures the frequency response of HF HRV versus the stimulus (breathing) and shows that phase varies monotonically with frequency and its value is approximately 0 at  $6\text{min}^{-1}$ .

## 3 RSA adaptive filtering

In the previous section discussed that, RSA reflects breathing pattern and RSA frequency varies as breathing pattern rate changes. Moreover, RSA amplitude is also a function of various variables, among them, the tidal volume. This condition makes adaptive filtering technique a fitting choice for the removal of RSA from HRV signal or in other word,

the separation of LF HRV and HF HRV from each other. In this way, RR interval is considered as the main signal and  $V_t$  plays the role of the reference signal in adaptive filtering system.

To make the case ready for adaptive filtering, signal pre-processing should be undertaken. It should be noted that the measured breathing pattern has a mean and also is not a pure sinusoid and conveys some of its fundamental frequency harmonics, while RSA frequency is believed to be related just to the fundamental frequency of  $V_t$ . Therefore, to have an efficient reference signal, in advance, these two unrelated components of the  $V_t$  signal have to be removed. Because of adequate distance between the harmonics band and the LF HRV band, a low order ordinary filter can handle the job. This may also be true for RSA that also conveys its harmonics, so the same band pass filtering for the RR interval is also recommended.

Another important condition that there exist is the variable phase shift between the RSA and the  $V_t$  that should be carefully regarded and its deteriorating impact on adaptive filter performance to be considered.

### 3.1 FIR Model based adaptive filtering

In order to separate the LF and HF components of an RR interval signal, prior to spectral analysis, the RR interval ( $R_R$ ) and the tidal volume ( $V_t$ ) signals are applied to an adaptive filter with FIR model shown in Fig.1.

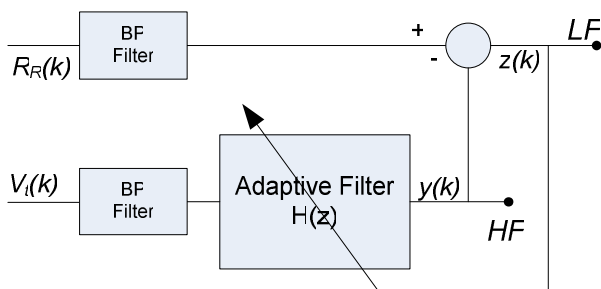


Fig.1. Adaptive filter based on an FIR model.

In this,  $H(z)$  is an FIR tunable filter as follows:

$$y(k) = \sum_{i=0}^{N-1} w_i V_t(k-i) \quad (1)$$

where  $W=[w_0, \dots, w_{N-1}]$  is its parameter vector,  $V_t(k)$  is input and  $y(k)$  is its output.

For  $H(z)$  to be able to predict the trace of  $V_t$  existing in the input  $R_R$  signal, namely RSA, the Least Mean Squares (LMS) algorithm is used. The LMS algorithm renders a set of optimum coefficients,  $W$ ,

which are adjusted so that the mean squared error (MSE) between the RSA and the predicted one,  $y(k)$ , is minimized.

In LMS, the weights are updated on a sample-by-sample basis as follows:

$$W_i(k+1) = W_i(k) + 2\mu V_t(k-i)[R_R(k) - y(k)] \quad (2)$$

$$i = 0, \dots, N-1$$

where  $N$  is the filter order. This is a practical approach to obtaining estimates of the filter weights ( $W$ ) in real-time without having to perform extensive computations. The algorithm does not require prior statistical knowledge of the signal and instead uses instantaneous estimates. Therefore, the weights obtained by the LMS algorithm are estimates that gradually improve over time as the filter weights are adjusted as the filter learns the characteristics of the signal, and eventually converge.

In the implementation, the set of weights is first initialized to zero. Then, for each subsequent sampling instants  $k$ , the filter output is computed using the FIR filter expressed by Eq. (1), where the output  $y(k)$ , predicting the respiratory or RSA component in the RR interval signal, is the filtered tidal volume ( $V_t$ ). Having the predicted RSA, it is now possible to linearly subtract it from RR interval signal,  $R_R$ . The error estimate is the algorithm output and is computed by:

$$z(k) = R_R(k) - y(k)$$

where  $z(k)$  is the LF component and  $y(k)$  is the predicted HF or RSA component. The filter weights  $W$  are updated based on this error expressed by Eq.(2), where  $\mu$  controls the rate of convergence and the stability of the algorithm.

### 3.2 The proposed model

Having a close look at the oscillatory nature of the two signals,  $V_t(k)$  and  $R_R(k)$ , it directs us to a better model structure for adaptive filter. If it is assumed that most of the  $R_{SA}(k)$  power resides in its fundamental frequency, as it is the case, the stirring part of  $V_t(k)$  can be modeled by a cosine function,

$$V_t(k) = A \cos(\omega k)$$

Then, its trace in the RR interval,  $R_{SA}(k)$ , will also be a type of shifted cosine with certain amplitude,

$$R_{SA}(k) = B \cos(\omega k - \varphi)$$

For exact cancellation of  $R_{SA}(k)$  from  $R_R(k)$ ,  $y(k)$  has to be,

$$y(k) = B \cos(\omega k - \varphi)$$

For the estimation of the  $R_{SA}(k)$ , the reference signal,  $V_r(k)$  is passed through an adaptive filter and eventually, it is expected that the output,  $y(k)$  to be a correct estimate of  $R_{SA}(k)$ .

In this paper, by using a different expression,  $y(k)$  is generated out of  $V_r(k)$  by introducing a new fit to case concept. In this method,  $y(k)$  is formed by summation of  $V_r(k)$  with its arbitrary shifted version. The reason behind that comes out of this simple argument that a shifted version of a sinusoid can be attained by summation of two different phase shifted sinusoid as follows:

$$\alpha_1 [ A \cos(\omega k) ] + \alpha_2 [ A \cos(\omega k - \delta) ] = B \cos(\omega k - \varphi)$$

This can also be written in vector form,

$$\alpha_1 [ A e^{j0} ] + \alpha_2 [ A e^{-j\delta} ] = B e^{-j\varphi}$$

The solution to the equation is,

$$\alpha_1 = \frac{B \sin \varphi}{A \sin \delta} \quad \alpha_2 = \frac{B \sin(\delta - \varphi)}{A \sin \delta}$$

The solution does not set a specific value for  $\delta$ , except that it must be nonzero.

This type of model can also be expressed in geometrical concept. A cosine function can be represented by a vector, where its angle equals to the cosine phase shift. Since in a plane, any vector can be formed by summation of two out of phase variable length vectors (with probable minus sign), any shifted phase cosine can also be generated by summation of two different phase shifted cosine.

The way that this idea is accommodated in adaptive filtering is shown in Fig. 2.

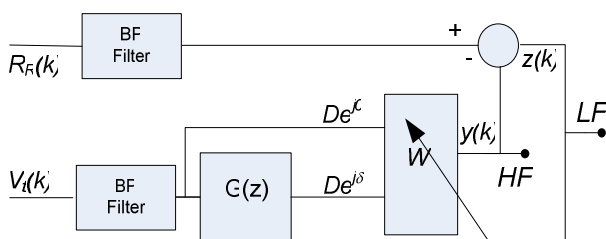


Fig. 2. Adaptive filter with a special model.

In this structure, input  $V_r$  is injected into the algorithm through two branches. From the first branch, it directly enters and forms vector 1,  $V_r = D e^{j0}$ , that is in phase with  $V_r$ . From the second branch, vector 2,  $V_{rd} = D e^{j\delta}$ , is formed that is a phase shifted version of  $V_r$ . To do so,  $V_r$  is passed through a known allpass filter,  $G(z)$ :

$$G(z) = \frac{z^{-1} - \beta}{1 - \beta z^{-1}}$$

This filter has unity amplitude and inserts necessary phase shift in the input signal, so that  $V_r = D e^{j0}$  is transformed to  $V_{rd} = D e^{j\delta}$ . Then the two branches enter the tunable parameter block and summed together.

$$y = w_0 V_r + w_1 V_{rd}$$

This output provides the desired shifted version of  $V_r$  needed for subtraction from RR interval to remove RSA from  $R_R(k)$  interval. This is achieved, once the weights will have been properly adjusted.

Figure 3 shows an example of the involved signals. The dotted line is the reference signal, the dashed line is the arbitrary shifted one and the solid line is the output of the above mentioned idea that has been fully settled over the desired signal.

The choice of  $\beta$  alters the rate of convergence of the underlying LMS algorithm. Our Experiments support this proposition.

Noting that by setting  $\beta=0$ , the proposed scheme turns to the conventional adaptive filter. Therefore, one conclusion may be that, a first order FIR model adaptive filter (which has 2 parameters) can also be able to filter the signal adequately. To examine the case, the following experiments are conducted.

The  $V_r$  signal is assumed to be,

$$V_r(k) = A \cos(2\pi * 0.15k)$$

and then  $R_{SA}(k)$  will be,

$$R_{sa}(k) = A \cos(2\pi * 0.15k - \pi/2)$$

In the first experiment, a second order FIR filter was used. The result of the test has been depicted in Fig. 4. After 100 seconds, the algorithm has still not fully converged. This result obtained with maximum possible value of  $\mu=0.25$ . The upper graph shows, how two parameters of the filter are changing to accommodate the situation.

In the next trial the order of  $N=4$  is assigned to the FIR model with  $\mu=0.1$ . Figure 5 shows the results: the lower graph, the error in the estimation

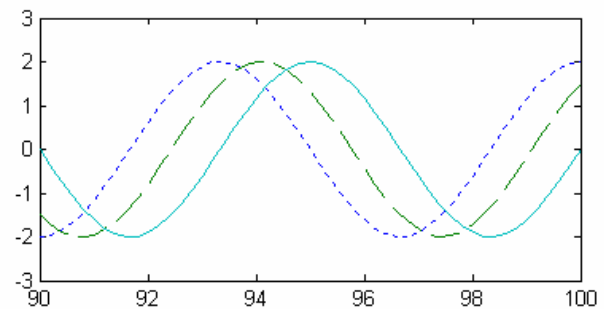


Fig. 3. Generating an estimate of a shifted sinusoid  $R_{SA}(k)$ (solid line) from  $V_r$  (dotted line) and its arbitrary shifted version,  $V_{rd}$ ( dashed line).

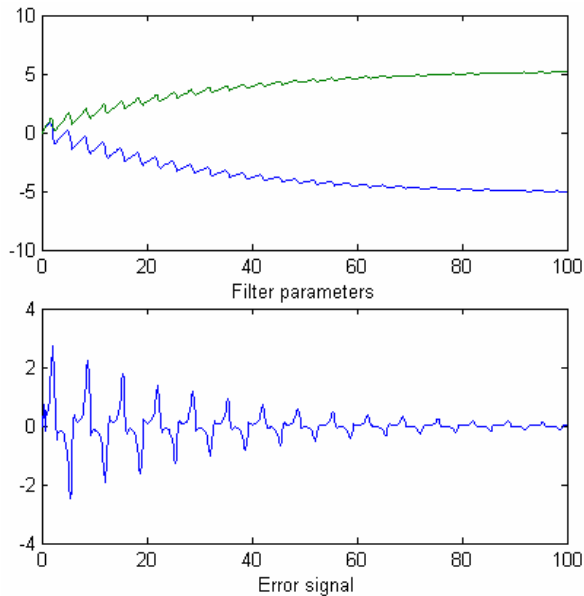


Fig. 4. The performance of the FIR model adaptive filter with  $N=2$ .

and the upper graph, the trace of 4 filter parameters. This time it took about 20 second for the algorithm to converge.

In the third experiment an 8 order FIR filter with  $\mu=0.02$  was tested. Figure 6 illustrates the results. Convergence happens after 10 seconds and 8 parameters of the filter change appropriately to manage the situation.

In the last experiment, the signals are applied to the proposed model. The rate of convergence of the algorithm can be viewed from Fig. 7. From this figure, it can be clearly realized that It took less than 4 seconds for the algorithm to converge. This is the point that this paper tries to make much of it. Figure

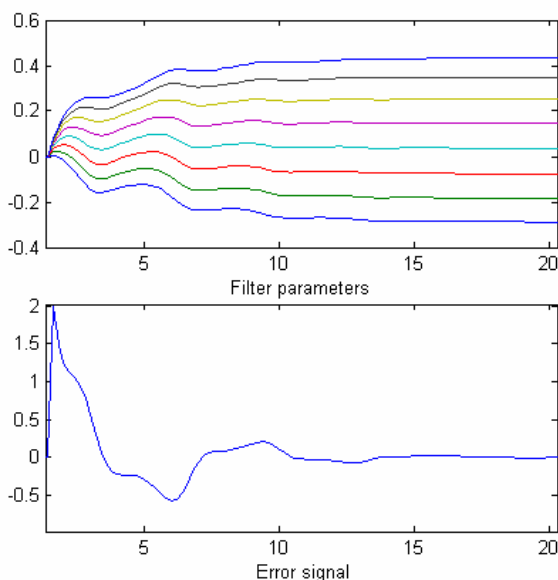


Fig. 6. The performance of an order 8 FIR model adaptive filter.

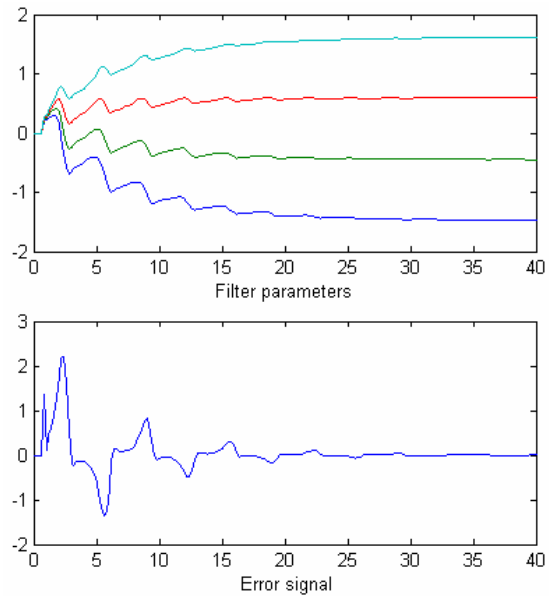


Fig. 5. The performance of the FIR model adaptive filter with  $N=4$ .

3 shows the  $V_t$  signal (dotted line), the phase shifted  $V_{td}$  and the produced  $y(k)$  (solid line) that has been resided over the  $R_{SA}(k)$ . Exact estimation of  $R_{SA}(k)$  has now been obtained in a shortest period.

Figure 7 clearly indicates the superiority of the suggested design to the other FIR choices. This result was obtained by setting  $\mu=0.25$  and  $\beta=0.6$ . Figure 8 is the same test with  $\beta=0.9$ , indicating that the sensitivity of the algorithm to the choice of  $\beta$  is low.

Changes of  $\beta$  affects the algorithm performance, therefore, it has to be set appropriately. Fortunately, in HRV filtering, the sensitivity of the algorithm to the value of  $\beta$  is low. For respiratory signal frequency between 0.15 to 0.4 Hz, real world span of the signal, and under various phase shifts, a value between 0.6 and 0.9 for  $\beta$  can fulfill the job. Search for an optimal value of  $\beta$  can easily be embedded in the LMS algorithm, but for this case is not really needed. No need to say that it adds to the complexity of the algorithm.

## 4 Simulations

### A. Data

The tidal volume data may be collected from the LifeShirt. The LifeShirt contains two inductive plethysmography (IP) sensors encircling the ribcage and abdomen used to measure tidal volume.

In this experiment, the harmonics and the mean of the  $V_t(k)$  and  $R_{SA}(k)$  are assumed to have been already filtered by a band pass filter. Noting that the

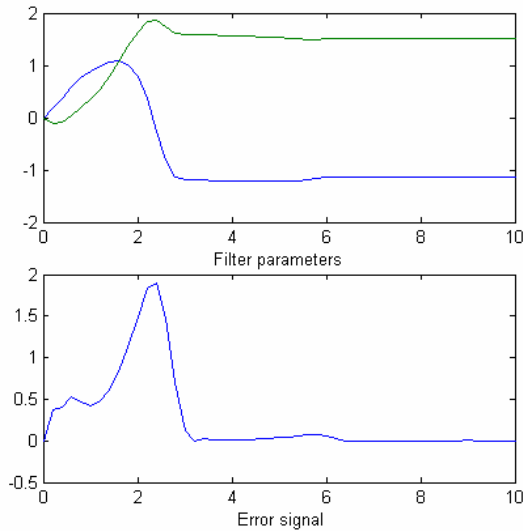


Fig. 7. The performance of the proposed model adaptive filter with  $N=2$  and  $\beta=0.6$ .

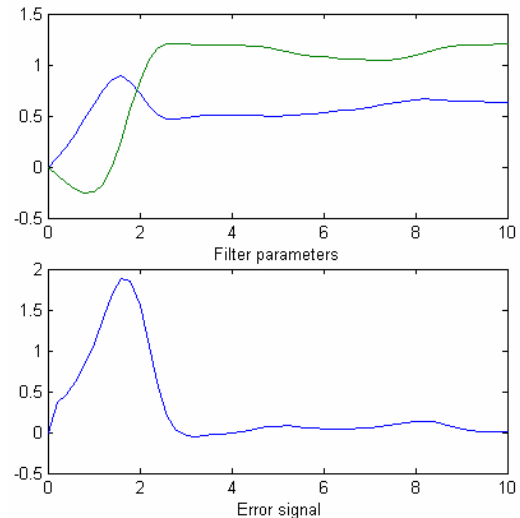


Fig. 8. The performance of the proposed model adaptive filter with  $N=2$  and  $\beta=0.9$ .

harmonics band is totally separated from the LF frequency band and there is not any overlapping between them to make filtering difficult. This beforehand filtering action, improves the performance of the adaptive filter methods. Actually, a third order Elliptic filter with pass band edge of 0.15Hz and stop band edge of 0.3Hz is adequate for harmonics cancellation and high frequency measurement noise reduction. A real  $V_t$  signal, before BP filtering, looks more like the graph in Fig.9 than a pure sinusoid. Its harmonics at 0.3 Hz has been illustrated in the spectrum graph.

On this basis, the BP filtered tidal volume simulation signal [5] can be written as,

$$Vt(t) = D \cos(2\pi f_h t) \quad (3)$$

where the volume is expressed by  $D$  whose value depends on ribcage and abdominal cross sectional area, which varies with changes in posture and mass.

The LifeShirt also contains a single lead ECG sampled at 200 Hz, which is linearly interpolated to 1 kHz, and heart rate is determined based on R wave locations.

The BP filtered RR interval simulated signal may be represented by [5]:

$$s(t) = A \sin(2\pi f_h t + \alpha_h) + B \sin(2\pi f_l t + \alpha_l) \quad (4)$$

where  $A$  is the peak-to-peak RSA amplitude per breath, expressed in msec,  $B$  is the LF/HF ratio, expressed as a fraction of  $A$ . The parasympathetic (HF) component and sympathetic (LF) component have frequencies  $f_h, f_l$  and phases  $\alpha_h, \alpha_l$  respectively. Based on the discussion in section 2, RSA component of  $R_R$  has the same frequency as  $V_t$  with a

variable phase shift. Both signals are assumed to be sampled in 5msec intervals.

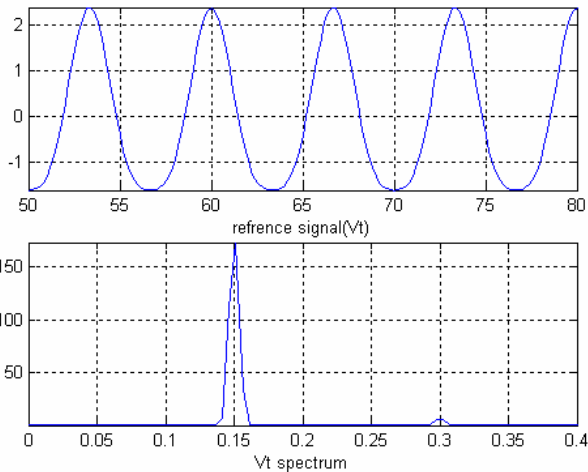
### B. FIR Model adaptive filter

The simulated RR interval signal, before BP filtering, has been illustrated in Fig. 10 for a parameter set with high and low frequencies of 0.15 and 0.13Hz, respectively, where power leaks from the LF band into the adjacent HF band.

No phase variation is applied to this signal. An RSA amplitude of  $A = 200$  msec is used with  $B=100$  to give a 50% LF/HF ratio. These signals are applied to the adaptive filter. Figure 11 shows the predicted HF component within the RR signal, predicted based of the reference signal  $V_t$ . It is evident from the trace that it takes approximately 100 seconds for the filter to tune and adapt to simulation characteristics. The weighting parameters are as follows:

$$W=[0.0013, 0.0241, 0.0460, 0.0662, 0.0840, 0.0987, 0.1098, 0.1169, 0.1199, 0.1186, 0.1131, 0.1036, 0.0905, 0.0744, 0.0558]$$

The LF signal is derived by linearly subtracting the HF signal from the original raw signal. Figure 12 shows the separated LF signal and its spectrum. It is obvious that the HRV has been accurately decomposed. These results are obtained with the filter order of  $N=15$ . Increasing the filter order does not improve the results as is the case with LMS. Decreasing it below  $N=6$ , leads to algorithm complete failure. The step size parameter,  $\mu=6 \times 10^{-4}$  produced the best result. This value appears to be very small, as the input signals have not been normalized. This is one drawback using the ordinary LMS adaptive filter, since when heart rate and

Fig. 9. A type of realistic  $V_t$  signal.

respiratory amplitude vary the updating parameter requires retuning. This is resolved with the Normalized Least Mean Squares NLMS, which is common in most software packages. This approach has been shown to increase accuracy when applied to current HRV spectral analysis techniques. However, when applying linear subtraction, although the predicted signal may be nearly perfect, any slight phase variation creates large artifact in the resultant signal [5].

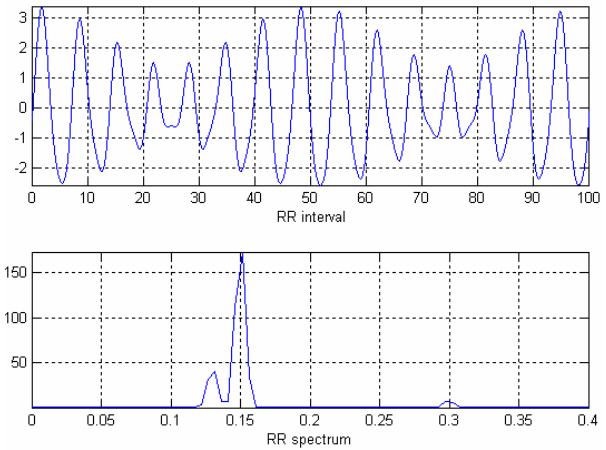
The graphs in Fig. 11 and 12 are the reproduction of the investigation reported in [5] done with an FIR model of order  $N=20$ . The frequencies of the test in here, are different from [5]. Apparently, the reason for using  $N=20$  in [5], as we noticed in our simulations, is due to the DC offset of  $V_t$  signal that would probably had not got removed.

### C. The proposed model adaptive filter

This time the simulated  $RR$  interval and  $V_t(k)$  signal are applied to the proposed model with  $\beta=0.8$ . Figure 13 and Fig. 14 show the results. The optimum filter parameters are:  $W=[-0.0693, 1.0442]$ . The acceptable result with  $\mu=25*10^{-4}$  is obtained.

As the graphs show, the proposed model having just two parameters, works analogous to the FIR filter with  $N=20$  as reported in [5] or FIR filter with  $N=15$  that we used for the reproduction of the results of [5].

What is important with this model, as our experiments indicate and the model structure suggests, is that this model is able to strongly tackle the phase shift variation given by  $\alpha_i$  changes, what a FIR model adaptive filter fails to accomplish easily. This is, of course, true for the studied case and for the other situations must be investigated.

Fig. 10. The simulated  $RR$  interval and its spectrum.

## 5 CONCLUSION

In this paper a new model structure for adaptive filtering, based on the nature of the involved signals, is introduced that gives similar performance as what a higher order FIR model adaptive filter in removing RSA component of HRV may yield. The trace of  $V_t$  signal in  $RR$  interval (RSA) is an unknown shifted phase  $V_t$  with, generally, unknown amplitude. On this basis, the proposed model is designed so that to have the capability of tracking the phase shifted  $V_t$ , and its probable variations, in the  $RR$  interval. This is accomplished by summing together  $V_t$  signal with its arbitrary shifted version through a set of optimally adjusted weights. It is shown that the proposed model significantly improves the rate of convergence of the underlying LMS algorithm. This strength is what makes the new model to perform superior to a high order FIR model adaptive system of HRV signal filtering.

**Acknowledgement.** This work was partially supported by ETRC, Shahed university, Tehran, IRAN.

### References:

- [1] M.H. Crawford, S. Bernstein, P. Deedwania, ACC/AHA guidelines for ambulatory electrocardiography. *Circulation* 100, 1999, PP. 886-893.
- [2] D.L. Eckberg, Sympathovagal balance: a critical appraisal. *Circulation* 96, 1997, PP. 3224-3232.
- [3] P. Grossman, M. Kollai, Individual differences in respiratory sinus arrhythmia, intra individual variations and tonic parasympathetic control of the heart. *Psychophysiology* 30, 1993, PP. 486-495.

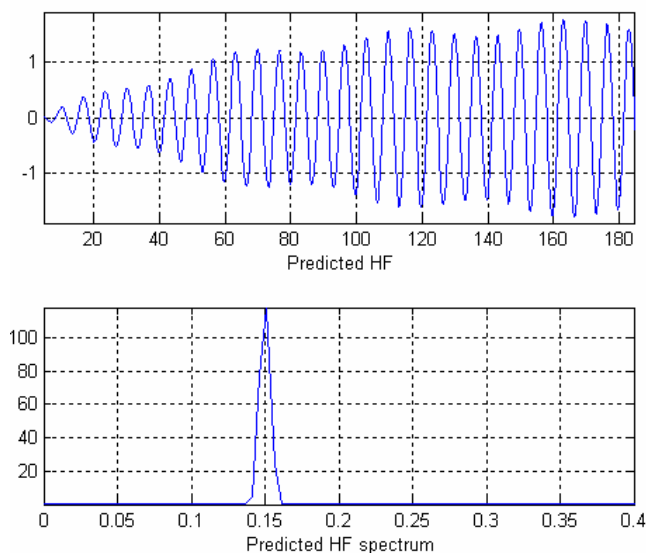


Fig. 11. Predicted HF by an order 15 FIR model.

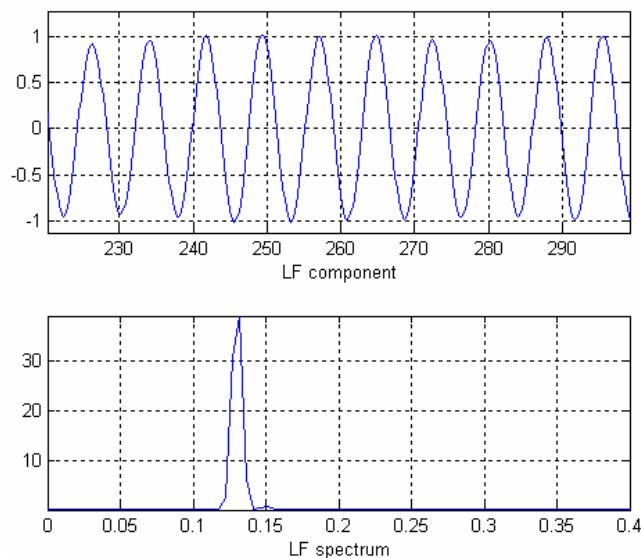


Fig. 12. Predicted LF by an order 15 FIR model.

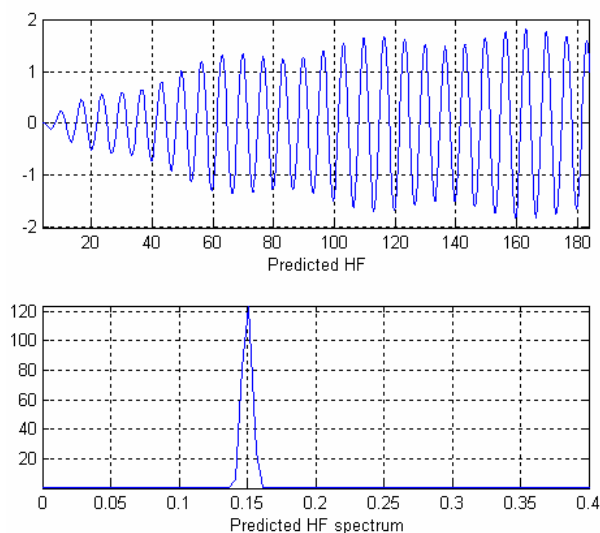


Fig. 13. Predicted HF by the order 2 proposed model.

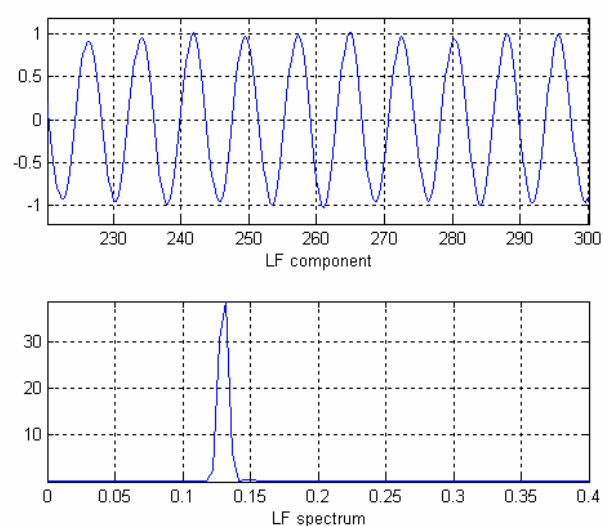


Fig. 14. Predicted LF by the order 2 proposed model.

- [4] P. Grossman, J.A. Van Beek, A Comparison of Three Quantification Methods for Estimation of Respiratory Sinus Arrhythmia. *Psychophysiology* 27, 1990, PP. 702-714.
- [5] D.B. Keenan, P. Grossman, Adaptive Filtering of Heart Rate Signals for an Improved Measure of Cardiac Autonomic control. *Int. J. of signal processing.* 2, 2005, PP. 52-58.
- [6] M. Pagani, N. Montano, A. Porta, Relationship between spectral components of cardiovascular variabilities and direct measures of muscle sympathetic nerve activity in humans. *Circulation* 95, 1997, PP. 1441-1448.
- [7] N. Sasano, A.E. Vesely, J. Hayano, H. Sasano, R. Somogyi, D. Preiss et al., Direct effect of PaCO<sub>2</sub> on respiratory sinus arrhythmia in conscious humans. *Am J Physiol Heart Circ Physiol* 282, 2002, PP. 973-976.
- [8] B.E. Shykoff, S.S. Naqvi, A.S. Menon, A.S. Slutsky, Respiratory sinus arrhythmia in dogs: Effects of phasic efferents and chemostimulation. *J Clin Invest* 87(5), 1991, PP. 1621-1627.
- [9] P. Robert, K. Daniel, Heart rate change as a function of age, tidal volume and body position when breathing using voluntary cardiorespiratory synchronization. *Physiol. Meas.* 18, 1997, PP. 183-189.
- [10] E. Vaschillo, B. Vaschillo, Lehrer P (2004) Heartbeat Synchronizes With Respiratory Rhythm Only Under Specific Circumstances. *Chest* 126, 2004, PP. 1385-1387.
- [11] K.K. Tripathi, Respiration And Heart Rate Variability : A Review With Special Reference To Its Application In Aerospace Medicine. *Ind J Aerospace Med* 48(1), 2004, PP. 64-75

- [12] H. Witte, U. Zwiener, M. Rother, S. Glaser, Evidence of a previously undescribed form of respiratory sinus arrhythmia (RSA)- the physiological manifestation of 'cardiac aliasing', *Pflugers Arch*, 412, 1988, PP. 442-444.
- [13] M.A. Garc'ia-Gonz'alez, C. V'azquez-Seisdedos, . Pall'as-Areny, Variations in breathing patterns increase low frequency contents in HRV spectra. *Physiol. Meas.* 21, 2000, PP. 417-423.
- [14] J.D. Schipke, M. Pelzer, G. Arnold, Effect of respiration rate on short-term heart rate variability. *J Clin Basic Cardiol* 2, 1999, PP. 92-95.
- [15] H. Kobayashi, Normalization of Respiratory Sinus Arrhythmia by factoring in Tidal Volume, *Journal of Physiological Anthropology*, 1998, PP. 207-213.
- [16] D. Laude, M. Goldman, P. Escourrou, J. Elghozi, Effect of breathing pattern on blood pressure and heart rate oscillations in humans *Clin. Exp. Pharmacol. Physiol.* 20, 1993, PP. 619-626
- [17] P. Grossman, F.H. Wilhelm, M. Spoerle1, Respiratory sinus arrhythmia, cardiac vagal control and daily activity, *Am J Physiol Heart Circ Physiol* 287, 2004, PP. 728-734.
- [18] G. Strauss-Blasche, M. Moser, M. Voica, D.R. McLeod, N. Klammer, W. Marktl, Relative timing of inspiration and expiration affects respiratory sinus Arrhythmia. *Clin Exp Pharmacol Physiol* 27, 2000, PP. 601-606.